Accepted Manuscript

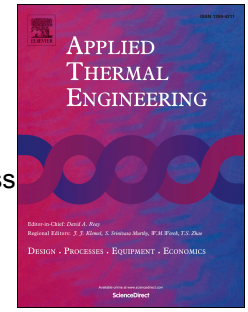

Influence of metallic porous microlayer on pressure drop and heat transfer of stainless steel plate heat exchanger

Jan Wajs, Dariusz Mikielewicz

PII: S1359-4311(15)00901-1

DOI: 10.1016/j.applthermaleng.2015.08.101

Reference: ATE 6990

To appear in: *Applied Thermal Engineering*

Received Date: 2 February 2015

Accepted Date: 28 August 2015

Please cite this article as: J. Wajs, D. Mikielewicz, Influence of metallic porous microlayer on pressure drop and heat transfer of stainless steel plate heat exchanger, *Applied Thermal Engineering* (2015), doi: 10.1016/j.applthermaleng.2015.08.101.

Influence of metallic porous microlayer on pressure drop and heat transfer of stainless steel plate heat exchanger

Jan WAJS *, Dariusz MIKIELEWICZ

Department of Energy and Industrial Apparatus, Gdansk University of Technology, ul. Narutowicza 11/12, 80-233 Gdansk, Poland, janwajs@pg.gda.pl, Dariusz.Mikielewicz@pg.gda.pl

* Corresponding author: Jan Wajs, Department of Energy and Industrial Apparatus, Gdansk University of Technology, ul. Narutowicza 11/12, 80-233 Gdansk, Poland, Email: janwajs@pg.gda.pl

Abstract The experimental analysis of passive heat transfer intensification in the case of plate heat exchanger has been carried out. The metallic porous layer was created on the heat transfer surface of analyzed unit. The experiment was accomplished in two stages. In the first stage the commercial stainless steel gasketed plate heat exchanger was investigated, while in the second one – the identical heat exchanger but with the modified heat transfer surface. The direct comparison of thermal and flow characteristics between both devices was possible due to the assurance of equivalent conditions during the experiment. Equivalent conditions mean the same volumetric flow rates and the same media temperatures at the inlet of heat exchangers in the corresponding measurement series. Experimental data were collected for the single-phase convective heat transfer in the water-ethanol configuration. The heat transfer coefficients were determined using the Wilson plot method. The results showed the advantages of such heat exchanger construction in some flow ranges and for some fluids.

Keywords: Porous microlyaer, Roughness increase, Heat transfer intensification, Plate heat exchanger, Pressure drop, Wilson plot method

Nomenclature

A - surface (m^2)
C - constant of linear regression
b - corrugation depth (m)
D_H - hydraulic diameter (m)
f - friction factor (-)
g - gravitational constant (m/s^2)
G - mass flux ($kg/(m^2s)$)
l - sampling length (m)
L - distance, width (m)
$\dot{m}$ - mass flow rate (kg/s)
P - pressure (Pa)
q - heat flux (W/m^2)
$\dot{Q}$ - rate of heat (W)
R - roughness parameter (μm)
Re - Reynolds number (-)
T - temperature (°C)
U_0 - overall heat transfer coefficient ($W/(m^2K)$)
$\dot{V}$ - volumetric flow rate (m^3/s)

Greek letters:

α - heat transfer coefficient ($W/(m^2K)$)
β - chevron angle (°)

Δ - difference value
λ - thermal conductivity (W/(mK))
μ - viscosity (Pa s)
ρ - density (kg/m^3)
φ - enlargement factor

Subscripts:
a - average arithmetical roughness
c - cold (ethanol)
exp - experiment
f - frictional
h - hot (water)
in - inlet
out - outlet
p - port
1Ch - one channel

1. Introduction

Nowadays we can observe a tendency to miniaturization in every field of life, but especially in technical applications. At the same time, in the area of energy technology very important are the problems of removal of high heat fluxes. This is the reason why the new challenges require high efficiency of system components, especially highly efficient and small volume heat exchangers. It is known that in the recuperator the heat transfer coefficients on both sides of partition are the most significant factors influencing the heat transfer surface and they determine its compactness. Because the overall heat transfer coefficient depends on the lower of the heat transfer coefficients values, a special care should be given to the heat transfer conditions on the "weaker" side in the heat exchanger.

Plate heat exchangers have been widely used in power engineering, chemical processes and many other industrial applications due to their good effectiveness and compactness. Nevertheless there are still investigations aiming at even more efficient and smaller size ones. They are going to be obtained by the heat transfer intensification and this new kind of plate heat exchangers could be prospectively applied for example in the heat recovery systems. Passive heat transfer enhancement can be obtained by changing the plate structure but also by changing the properties of utilized fluids. The first method will be discussed further in the present paper. The second method can be realized for example by application of nanofluids [1], but it is beyond the scope of these investigations.

General overview of heat transfer (in the flow passages) augmentation by passive methods can be found in literature (Gupta and Uniyal [2]), while Stone [3] concentrated on the heat transfer intensification in compact heat exchangers. He presented the methods of augmentation assessment by various parameters, followed by the overview of heat exchangers geometries including many kinds of fins, wavy and corrugated channels, etc. Comprehensive overview of recent advances in plate heat exchangers is presented by Abu-Khader [4]. Research connected with corrugated plate heat exchangers is undertaken in many directions. It may be concentrated on the heat transfer coefficient and formulation of heat transfer correlation (Khan et al. [5]), on the pressure drop and friction factor correlation (Arseneyeva et al. [6]), or both of them (Dovic et al. [7]). It can be done experimentally or numerically as presented by Islamoglu and Parmaksizoglu [8,9]. In many cases the researchers are looking for optimal geometry, causing heat transfer increase and possibly small pressure drop. To all mentioned above papers can be added a paper describing experimental investigation by Naik and Matawala [10], which in a general idea is very similar to this paper. They

examine single phase chevron type gasketed plate heat exchanger with oil-water heat transfer in dependence on flow rate, geometry, temperature conditions, etc. and compare the results with published correlations. There is one main difference with the present study – the surface roughness was not considered.

Therefore, although a large number of the plate heat exchangers investigations were reported in the professional literature, rather limited data for units with high performance microsizes, enhancement structures were available. Among them could be found works by Furberg et al. [11]. Their aim was to enhance pool boiling heat transfer of R134a by over one order of magnitude in comparison with a plain machined copper surface. They presented an experimental study of the plate heat exchanger evaporator performance with and without this novel enhancement structure applied to the refrigerant channel.

Müller-Steinhagen [12] described and analyzed a heat exchanger with a vacuum plasma sprayed 250 µm thick layer of spherically shaped Inconel 625 particles on to a plate and frame heat surface. The particles of 105–170 µm diameter enhanced the boiling heat transfer coefficient of R134a by up to 100%.

The influence of artificial roughness shape on heat transfer enhancement in the case of plate heat exchanger was published by Garcia et al. [13]. They investigated influence of three various roughness shapes (corrugated tubes, dimpled tubes and wire coils) on heat transfer and pressure drop in the laminar, transition and turbulent flow regions. In their case the roughness influence on the pressure drop exceeded the influence on heat transfer and they explained it by changing of the flow character from laminar to transition and then to turbulent. They recommended the Reynolds number regions for which analyzed by them geometries were the most suitable.

The experience connected with the passive heat transfer enhancement in the case of plate heat exchangers was also presented by Wajs and Mikielewicz [14]. Authors proposed a new technique of increasing the surface roughness, through abrasive blasting with the utilization of glass micro-beads. Granulation size of the beads was approximately 300-400 µm. Such technique is relatively cheap and still produces the enhancement effect. They conducted the series of experiments for water-water case comparing the commercially available heat exchanger with the modified surface heat exchanger. The thermal analysis showed that the overall heat transfer coefficient for the highest value of hot water mass flux was higher for the commercial heat exchanger than for the modified one. On the other hand, for the lowest value of hot water mass flux the opposite tendency was found. Within these limits (the highest and the lowest values of mass flux) there was the transient range, as named by the authors, where the overall heat transfer coefficient for some values of heat flux was higher for the commercial heat exchanger, for the other – higher for the modified heat exchanger. This tendency was observed by the authors for the first time but was also found for the different inlet temperature conditions of heat exchangers.

In this paper the experimental analysis of passive heat transfer intensification in the case of model plate heat exchanger has been presented for water-ethanol configuration. The passive intensification was obtained by a modification of heat transfer surface, which was this time covered by a metallic porous microlayer. As previously, the experiment was done in two stages, for two heat exchangers, that is the commercial stainless steel gasketed one and the identical heat exchanger but with the modified heat transfer surface. Experimental data were collected for the single-phase convective heat transfer in the water-ethanol configuration. The heat transfer coefficients were determined using the Wilson plot method.

2. Plate heat exchanger (PHE)

The model of corrugated plate heat exchanger (PHE) offered at the commercial market was the subject of presented investigations. In the considered heat exchanger the heat is transferred in one pass. The PHE model was made of stainless steel 316 according to AISI standard and consisted of

three plates, with thickness of each one of 0.5 mm. The surface roughness of working plate was equal to 0.46 μm (parameter R_a) and 3.36 μm (parameter R_z), respectively. Definition of the parameters will be explained later. The total length of the heat exchanger was 450 mm, while the overall heat transfer area was equal to 0.039 m^2. The distance between the plates was kept constant and the EPDM seal was fixed in the "hang on" system. Permissible working pressure was equal to 1.6 MPa. The schematic view of heat exchanger plate is presented in Fig. 1. The geometric details of tested corrugated plate are listed in Table 1.

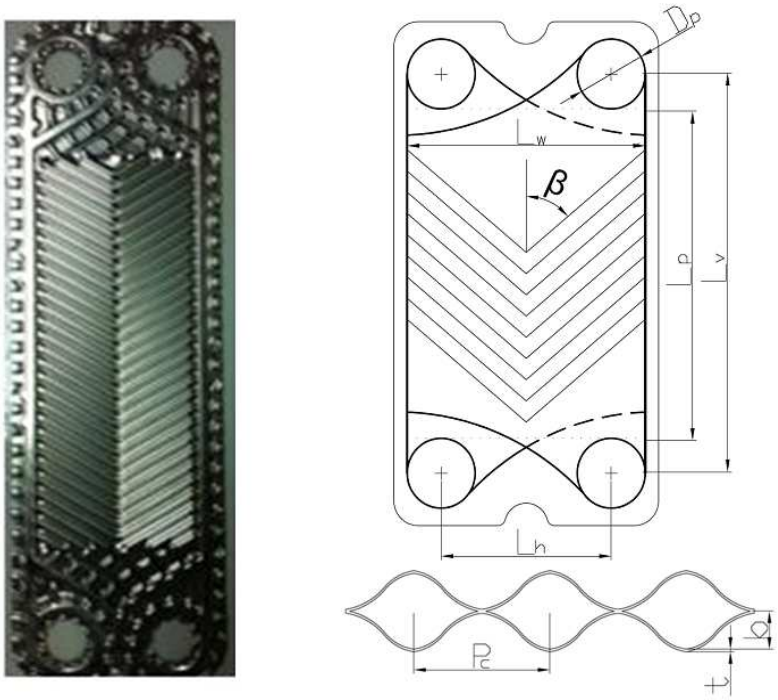

Fig. 1. Photography and schematic view of the original heat exchanger plate with characteristic parameters

To meet the needs of experiment in the second stage the porous layer was created on the heat transfer surface. The special metal finishing was applied to increase the surface roughness. As an abrasive agent the broken alundum with 500 μm average grain size was used. The alundum grains were carried by the stream of compressed air under the pressure of 0.6 MPa. This metal finishing increased the surface roughness about three times in comparison with the original plate.

The roughness changes of heat exchanger plate surface were examined by the Ship Design and Research Center in Gdansk [15]. The measurements were done with the Surftest 211 (Mitutoyo). After the calibration procedure done with application of the roughness' standard 178-601, delivered by Mitutoyo company, the flat parts of heat exchanger plates were examined. The sampling length was 0.25 mm. The results are presented in Table 2 with the following notation: "Before" – primary surface state, "After" – surface after the metal finishing. Parameter R_a is an average arithmetical roughness in the range of sampling length l (Fig.2). Parameter R_z is an arithmetic average of absolute height of five the highest roughness' peaks and height of five the deepest valleys in the range of sampling length l (Fig. 3).

Table 1. Characteristic dimensions of chevron plate used in the studies

chevron angle, β (°)	60
corrugation depth, b (mm)	3
corrugation pitch, P_c (mm)	8
plate thickness, t (mm)	0.5
plate width, L_w (mm)	98
vertical distance between ports centers, L_v (mm)	381
horizontal distance between ports centers, L_h (mm)	70
port to port length, L_P (mm)	353
effective area, A (m^2)	0.039
projected surface area, A_{wp} (m^2)	0.0346
enlargement factor, φ	1.127
port diameter, D_p (mm)	28

Table 2. Results of surface roughness measurement

sample	measured parameter	average value [μm]
Before	R_a	0.46
	R_z	3.34
After	R_a	1.43
	R_z	11.02

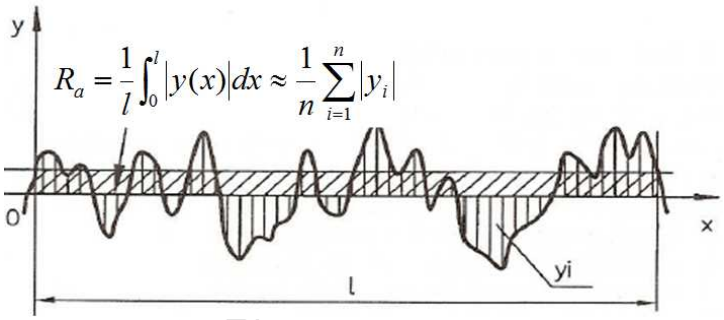

Fig. 2. Formula and graphical representation of parameter R_a

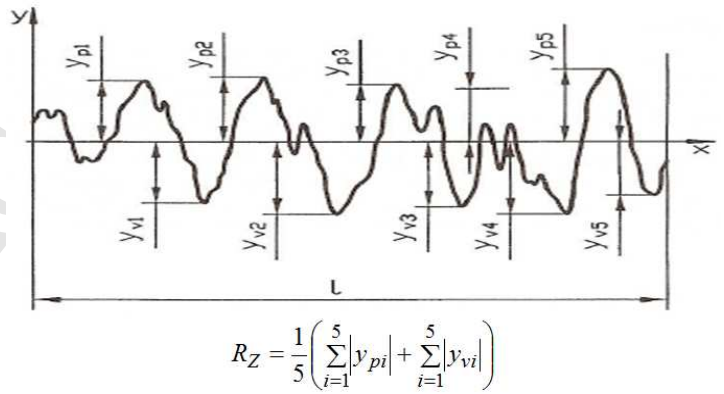

Fig. 3. Formula and graphical representation of parameter R_z

3. Experiment

The test facility, shown in Fig. 4, enabled the thermal-hydraulic investigations of convection between the hot water and ethanol. Water was the heating medium, while ethanol - the coolant.

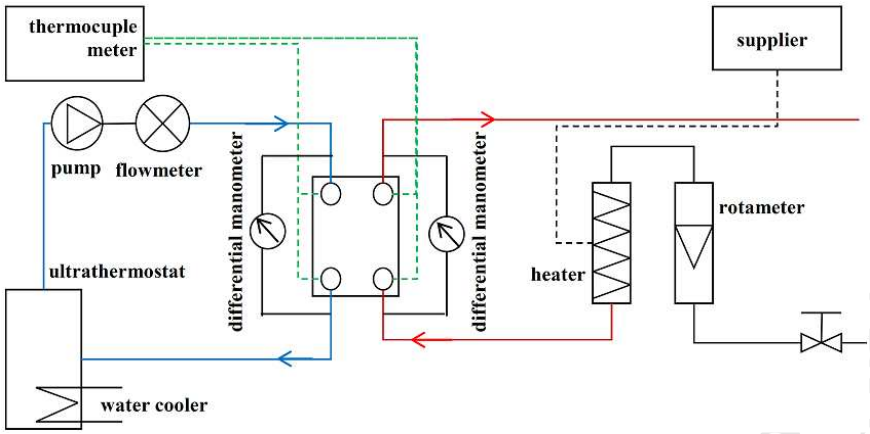

Fig. 4. Scheme of experimental facility

The water stream was at first directed to the rotameter and then to the electrical heater to obtain required parameters at the inlet of heat exchanger. The heater was controlled by the autotransformer, which allowed a smooth change of heater power and in consequence the precise water temperature settings.

The ethanol was circulating in a closed loop equipped with the thermostatic bath, which heated it to a certain level before entering the heat exchanger. For the needs of experiment an additional heat exchanger, supplied with the tap water (cold) was inserted to the thermostatic bath. It enabled the removal of thermal energy from ethanol, what assured the steady state of the analysis.

Additionally, both sides (water and ethanol) were equipped with the filters to ensure a purity of the media and to prevent fouling. As it is known, fouling can introduce a significant influence on the heat transfer performance [16].

During experiments the mass flow rate of hot water was varied in the range from 50 to 125 litres per hour (lph), while the ethanol mass flow rate in the range from 35 to 160 lph. Two levels of hot water temperature, supplying the heat exchanger, were tested namely 80°C and 60°C, whereas the ethanol temperature was kept constant in each measurement series and it was equal to 30±0.5°C.

The pressure drop was measured by the differential pressure transducer (Huba Control sensor) with accuracy of 1% of the full scale. Thermocouples of J-type were used to measure temperature in four locations i.e. at the inlet and outlet of heat exchanger cold side and at the inlet and outlet of heat exchanger hot side.

During experiments the following parameters were measured: the hot fluid temperature at the inlet ($T_{h\text{-}in}$) and at the outlet ($T_{h\text{-}out}$) of heat exchanger, the cold fluid temperature at the inlet ($T_{c\text{-}in}$) and at the outlet ($T_{c\text{-}out}$) of heat exchanger, pressure drop connected with the fluids flow (ΔP_{exp}) and volumetric/mass flow rate of working fluids. On the basis of measurement results the heat flux (q), the Logarithmic Mean Temperature Difference ($LMTD$) in the heat exchanger and the overall heat transfer coefficient (U_0) were calculated. The overall heat transfer coefficient was determined from the Peclet law based on the heat transfer area equal to 0.039 m^2 and average value of the rate of heat transferred through the wall in a given measurement series.

4. Heat transfer coefficient

Experimental investigations of heat exchangers seek determination of mean heat transfer coefficients on both sides of the wall separating heat exchanging fluids. Usually the procedure is to obtain direct temperature measurements on the heat transfer wall. However, if the heat exchanger has a complex geometry then accurate measurements of surface temperature faces significant difficulties. To attach the thermocouples at heat transfer surface, the heat exchanger has to be at first

disassembled and then reassembled. Special attention should be paid to the proper sealing and leakage prevention. The procedure is therefore tedious and not always successful. Some of difficulties can be alleviated if the Wilson plot method (Wilson [17]) is applied. The method is very simple and can be applied to the analysis of various types of heat exchangers (Fernandez-Seara et al. [18]). In effect the mean values of heat transfer coefficient can be obtained. A simple and efficient version of the Wilson plot method, similar to the original one, was applied in the course of present study of heat transfer coefficient. The original Wilson plot method, as well as its subsequent modifications, requires only determination of the overall thermal resistance in the heat exchanger. From this method an accurate energy balance, based on the measurement of fluids exchanging heat and their mean temperatures at the inlet and outlet from the heat exchanger are obtained.

The rate of heat in the heat exchanger can be presented in the form:

$$\dot{Q} = U_0 \cdot LMTD \cdot A = \dot{m}_h \Delta h_h = \dot{m}_c \Delta h_c \tag{1}$$

where LMTD denotes Logarithmic Mean Temperature Difference, A – heat transfer surface.The overall heat transfer coefficient can be described as:

$$U_0 = \left(\frac{1}{\alpha_h} + \frac{\delta}{\lambda} + \frac{1}{\alpha_c} \right)^{-1} \tag{2}$$

where α_h and α_c are heat transfer coefficients for respective mass flow rates, δ is the thickness of wall separating two fluids, whereas λ its thermal conductivity.

The log-mean temperature difference can be determined from a relation for the counter-current heat exchanger as:

$$LMTD = \frac{\left(T_{h\_in} - T_{c\_out}\right) - \left(T_{h\_out} - T_{c\_in}\right)}{\ln \dfrac{\left(T_{h\_in} - T_{c\_out}\right)}{\left(T_{h\_out} - T_{c\_in}\right)}} \tag{3}$$

Assuming that the heat transfer is primarily governed by the flow velocities of both fluids, the simple relations for determination of heat transfer coefficient as a function of fluid velocity can be written.

For $\dot{m}_c$ = const and $\dot{m}_h$ = var there is:

$$\alpha_c = const\,, \quad \alpha_h = C_h w_h^n \tag{4}$$

For $\dot{m}_h$ = const and $\dot{m}_c$ = var there is:

$$\alpha_h = const\,, \quad \alpha_c = C_c w_c^n \tag{5}$$

where w_h and w_c are the respective flow velocities of hot and cold fluids, n is the exponent depending on the flow character, for example in the case of turbulent flow inside tubes n=0.8.

For the heating medium the following relation can be formulated:

$$\frac{1}{U_0} = \left(\frac{1}{\alpha_c} + \frac{\delta}{\lambda} \right) + C_h w_h^{-n} \tag{6}$$

or:

$$\frac{1}{U_0} = C_3 + C_h w_h^{-n} \tag{7}$$

where:

$$C_3 = \frac{1}{\alpha_c} + \frac{\delta}{\lambda} \tag{8}$$

for a series where $\dot{m}_c$ = const. Assuming new variables, i.e. $x = w_h^{-n}$ and $y = 1/U_0$ a linear relation is obtained:

$$y = C_3 + C_h x \tag{9}$$

For cooling side analogical relations can be derived.

The heat transfer coefficient calculations by Wilson plot method were conducted for the plate thickness of 0.5 mm. The plate material (stainless steel) has the thermal conductivity λ equal to 15 W/(mK). The function described by formula (9) was plotted in Fig. 5 for the modified and commercial heat exchangers, respectively. Both lines represent the case, when the cooling fluid had a constant volume flow rate with a variable one for heating fluid. The inlet temperature of heating medium was equal to 80°C, while that of cooling one was 30°C. The constants in equation (9) have been determined and feature the following values: C_h=33×10^{-6} and C_3=25×10^{-5} (for modified heat exchanger) and C_h=26×10^{-6} and C_3=30.6×10^{-5} (for commercial one).

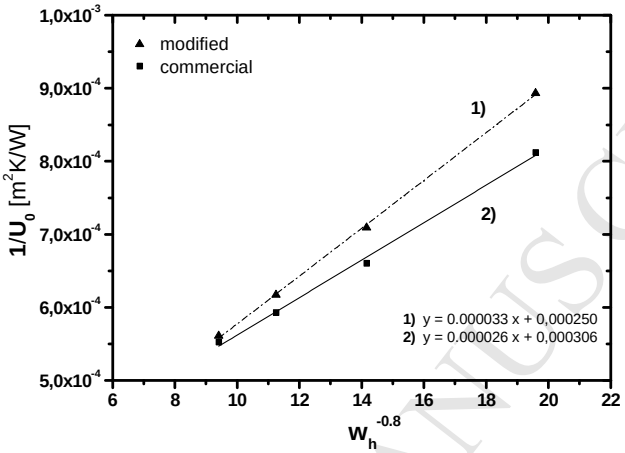

Fig. 5. Experimental points and the corresponding linear regression, $\dot{V}_C$ = 125 lph

It should be mentioned that each function presented in Fig. 5 was used to calculate just one point representing the heat transfer coefficient of cooling medium. All calculated values of heat transfer coefficient for both media are shown in Figs. 6 and 7. These figures were constructed on the basis of numerous linear functions similar to those presented in Fig. 5.

The heat transfer coefficient values obtained for the hot and cold passages are shown in Figs. 6 and 7. Their values are plotted versus Reynolds number for one chevron channel (as usually presented in the papers). During tests the inlet temperature of hot water and ethanol (cooling fluid) was kept constant (see the legend of figures).

The Reynolds number for one flow channel was calculated with application of the formula:

$$\mathrm{Re}_{1Ch} = \frac{G_{1Ch} D_H}{\mu} \tag{10}$$

where hydraulic diameter, D_H, has been defined in the same way as in similar studies:

$$D_H = \frac{2b}{\varphi} \tag{11}$$

In Eq. (11) b is the corrugation depth and φ is the enlargement factor.

The enlargement factor φ was calculated in accordance with [5] as a ratio of particular plate areas:

$$\varphi = \frac{A}{A_{wp}} \tag{12}$$

where A is the effective corrugated area of plate, whereas A_{wp} its projected surface.

The projected surface area is related to geometrical characteristics of the plate and was determined as follows:

$$A_{wp} = L_w \cdot L_p \tag{13}$$

where L_w is the plate width and L_p is the port to port length calculated by subtracting the port diameter from vertical distance between ports centers (also called active length of heat exchanger):

$$L_p = L_v \cdot D_p \tag{14}$$

The viscosity of both fluids was calculated using Refprop 9.0 [19] software for the average temperature of hot passage ($T_{h\text{-}in}$+$T_{h\text{-}out}$)/2 and cold passage ($T_{c\text{-}in}$+$T_{c\text{-}out}$)/2 in the heat exchanger, respectively. The one channel mass flux, G_{1Ch}, was determined using the following definition:

$$G_{1Ch} = \frac{\dot{m}}{b\,L_w} \tag{15}$$

In Eq. (15) $\dot{m}$ is the fluid mass flow rate, b is the plate corrugation depth, whereas L_w is the plate width.

As results from the analysis of Fig. 6 in the case of commercial and modified surfaces, at the same conditions, the higher values of heat transfer coefficient were found on the ethanol side, than on the water side. When the inlet temperature of water was set to 80°C (Fig. 7), the improved heat transfer on the porous layer caused further considerable increase of the heat transfer coefficient on ethanol side. For example at the Reynolds number equal to 600, the heat transfer coefficient on the water side is 18% higher for the case of commercial module, while on the ethanol side it is 15% higher for the modified one. Summarising, ethanol at the same Reynolds number shows better heat transfer characteristics than water. With increasing the maximum temperature difference in the heat exchanger that heat transfer characteristic is even better.

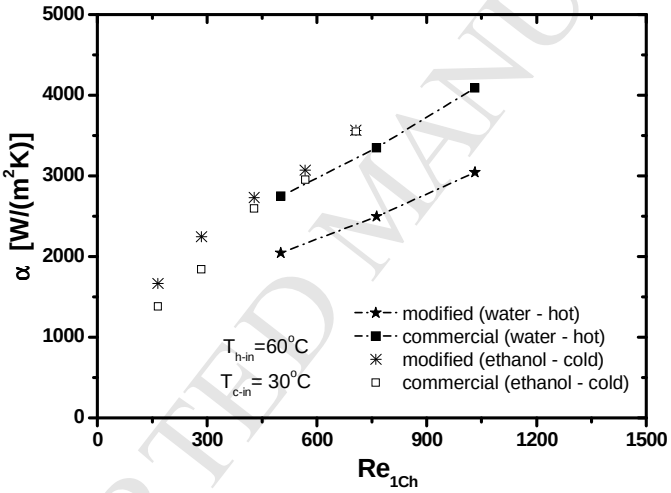

Fig. 6. Comparison of heat transfer coefficients versus the Reynolds number for the case of water – ethanol configuration; $T_{h\text{-}in}$ = 60°C

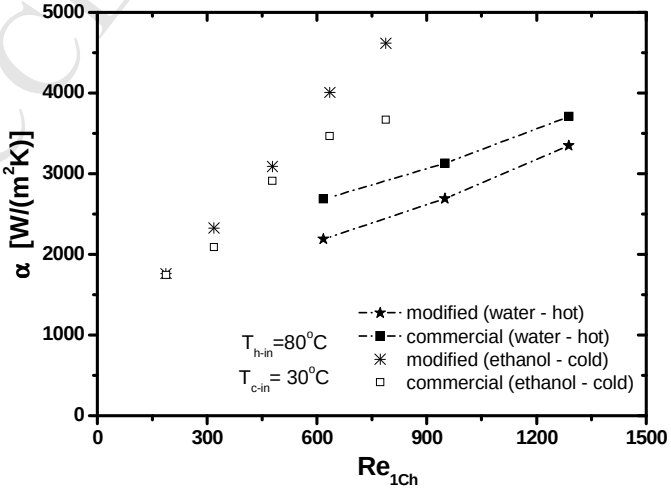

Fig. 7. Comparison of heat transfer coefficients versus the Reynolds number for the case of water – ethanol configuration; $T_{h\text{-}in}$ = 80°C

The explanation of above discussed results can be done in the basis of the roughness, fluid properties and flow structure. The surface tension can be connected with wettability and temperature which additionally influences the Prandtl number. The latter number contributes to differentiation between the hydrodynamic and thermal boundary layers. Wettability indicates the ability of a liquid to maintain contact with a solid surface [20]. Usually it is considered in the case of the presence of three phases. However in single-phase flow, there can be distinguished the hydrophobic and hydrophilic surfaces as well as the apparent slip flow [20]. Although the hydrophobic and hydrophilic surfaces are not the issue in the considered case, but an apparent slip flow can be considered in the light of the flow reattachment [21]. Let's consider a detachment of the flow on the single rough structure, then it impinges on the next structure. In such case we can observe appearance of the reverse flow in the small gap between them. For particular flow conditions the main stream will flow at the top of the roughness, that is why it can be called "apparent slip flow", since it would be in some distance from the wall. The depth of main stream penetration would be varying. It should be emphasized, that such phenomenon is not caused by the presence of non-condensable gases. The special care was taken to prevent air presence in the system during the experiment.

Since water is characterized by high values of surface tension, it can be assumed that on the heat exchanger water side the real heat transfer area is reduced by the size of non-penetrable roughness. That could probably explain why water exhibits lower values of heat transfer coefficient in relation to ethanol. The properties of water and ethanol are listed in Table 3.

Increasing difference between the heat transfer coefficients of the modified and commercial heat exchangers (see Fig. 6) can be also interpreted on the basis of Prandtl number and the thickness of boundary layers. At 60^{o}C the water Prandtl number was equal to 2.98. It means that the hydrodynamic boundary layer was thicker than the thermal one. Increasing Reynolds number causes reduction of boundary layer thickness, therefore the transport processes are enhanced, what can be observed in Figs. 6 and 7. However in the case of rough surface, due to "apparent slip flow" thinning of boundary layers were less effective and they were still not sufficiently turbulent. The situation has changed with the water temperature increase, which can be found in Fig. 7. For the water side the difference between the heat transfer coefficients of the modified and commercial heat exchangers decreased. At higher temperature the water surface tension and the Prandtl number are smaller, that is why the roughness became more important. The negative influence of the "slip flow" was reduced and also the boundary layers could be more effectively disturbed.

Considering the ethanol side of modified and commercial heat exchangers the tendency of data presented in Figs. 6 and 7 is in contrary to the water case. Ethanol has almost 3.5 times lower surface tension than water at 30^{o}C (Table 3). Due to that it penetrated easily the roughness and the "apparent slip flow" didn't occur. That is why the heat transfer coefficient was higher for the modified heat exchanger. This advantage was reduced by the increase of Reynolds number (Fig. 6). At 30^{o}C the ethanol Prandtl number is equal to about 16, it means that the hydrodynamic boundary layer was much thicker than the thermal one. It was also true in comparison to the case of water. Therefore destabilization of the hydrodynamic boundary layer could not be sufficient for higher increase of heat transfer coefficient. Moreover the probability of "slip flow" appeared, since the main stream could pass at some distance from the roughness bottom, where the reverse flow could be expected. This disadvantage disappeared or was strongly reduced at higher temperature (Fig. 7). Decreasing values of the surface tension and the Prandtl number, equivalent to disappearance of "apparent slip velocity" and at the same time to reduction of boundary layers size, caused significant increase of heat transfer coefficient on the ethanol side.

5. Thermal characteristics

The exemplary comparison of studied heat exchangers thermal characteristics are shown in Figs. 8-9. Direct comparison of the thermal and flow characteristics between both devices was possible due to an assurance of equivalent conditions during the experiment. Equivalent conditions mean the same volumetric flow rates and the same media temperatures at the inlet of heat exchangers in the corresponding measurement series.

Table 3. Thermophysical properties of water and ethanol

medium	water			ethanol		
temperature ^{o}C	30	60	80	30	40	50
surface tension mN/m	71.19	66.24	62.67	21.14	19.87	18.65
Prandtl number	5.41	2.98	2.22	15.85	14.01	12.45

The effect of water mass flux and imposed heat flux on the overall heat transfer coefficient in the studied plate heat exchangers are presented in Fig. 8 and Fig. 9. The presented graphs were constructed at the following conditions: temperature of hot water at the heat exchanger inlet was 60°C, while temperature of ethanol at the heat exchanger inlet was 30°C, the mass flux of hot water (G_h) was kept constant and its value is indicated in particular figures. The Reynolds number value represents variable ethanol mass flow rate.

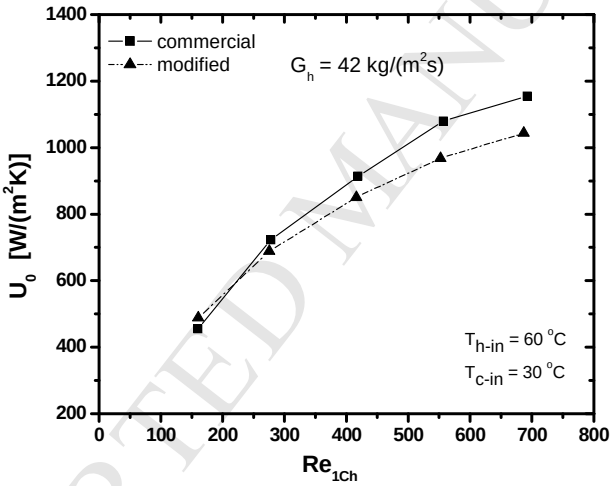

Fig. 8. Overall heat transfer coefficient versus the ethanol Reynolds number in the water – ethanol configuration, the water mass flux G_h = 42 kg/(m^{2}s)

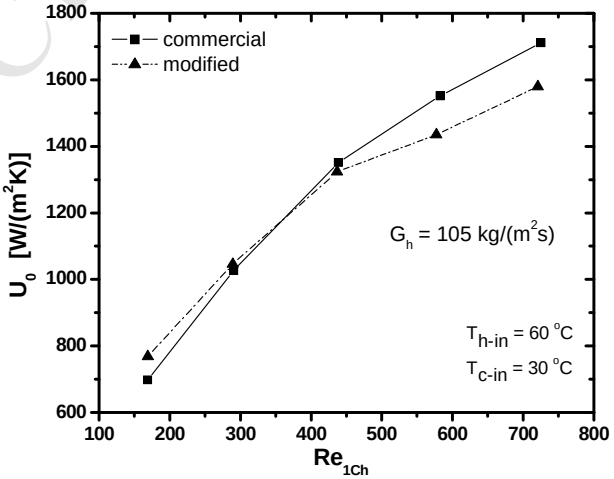

Fig. 9. Overall heat transfer coefficient versus the ethanol Reynolds number in the water – ethanol configuration, the water mass flux G_h = 105 kg/(m^{2}s)

The results in Figures 8 and 9 can be divided into two parts: namely the low Reynolds number region (up to about 300) and the higher Reynolds number region (over 300). This division is coming from the fact, that in the low Reynolds number region the overall heat transfer coefficient was higher for the case of modified heat exchanger than for the commercial one of about 2 to 10%. The difference was calculated based on the following formula in assumption that the value for commercial heat exchanger is the reference one:

$$\Delta U_0 = \frac{\left| U_{0\_commercial} - U_{0\_modified} \right|}{U_{0\_commercial}} \cdot 100\% \tag{16}$$

On the other hand, in the higher Reynolds number region the commercial heat exchanger was characterized by higher values of the overall heat transfer coefficient (by about 6% to 10%) than the modified one. Such tendency was observed for both cases of mass flux, equal to 42 and 105 kg/(m^{2}s). Calculated values of overall heat transfer coefficient for both heat exchangers are presented in Table 4.

Table 4. The overall heat transfer coefficient difference between the modified and commercial heat exchanger

heat exchanger	commercial		modified		
	U_0[W/m^{2}K]	Re	U_0[W/m^{2}K]	Re	ΔU_0[%]
Water mass flux	1155	692	1044	687	9.6
G_h = 42 kg/(m^{2}s)	1080	557	968	552	10.3
	914	419	851	416	6.9
	723	278	688	276	4.8
	456	160	488	160	7
Water mass flux					
G_h = 105 kg/(m^{2}s)	1712	725	1580	721	7.7
	1552	583	1436	577	7.5
	1351	438	1324	437	2
	1026	290	1046	289	2
	698	169	769	169	10.2

Similar results were obtained for the measurement series, in which temperature of hot water at the heat exchanger inlet was equal to 80°C and temperature of ethanol at the heat exchanger inlet was equal to 30°C.

6. Hydraulic characteristics

Generally, the total pressure drop (ΔP_{exp}) consists of four factors namely the frictional term (ΔP_f), elevation term (ΔP_g), pressure losses at the test section inlet and outlet ports (ΔP_p), and the acceleration term (ΔP_a). The last term would be included in the analysis only if the phase change of particular fluid could be observed. Therefore in the case of reported study, the acceleration term was omitted because there was no phase change. The gravitational component was not taken into account due to the horizontal position of heat exchangers. To evaluate the friction factor associated with the water flows, the frictional pressure drop (ΔP_f) was calculated by subtracting the pressure losses at the ports of heat exchanger from the measured total pressure drop:

$$\Delta P_f = \Delta P_{\exp} - \Delta P_p \tag{17}$$

The pressure drop at the inlet and outlet ports of heat exchanger was empirically suggested by Shah and Sekulic [22]. This is approximately 1.5 times the head due to the flow expansion at the

inlet:

$$\Delta P_p \approx 1.5\left(\frac{G_p^2}{2\rho}\right) \tag{18}$$

where ρ is the density of fluid, and G_p, is the mass flux inside the port, defined as:

$$G_p = \frac{4\dot{m}}{\pi D_p{}^2} \tag{19}$$

In Eq. (19) D_p is the port diameter.
The friction factor is described by formula:

$$f = \frac{\Delta P_f D_H \rho}{2 G_{1Ch}{}^2 L_p} \tag{20}$$

where L_p is the active length of heat exchanger.
The flow characteristics are presented in Fig. 10 (for water side) and Fig. 11 (for ethanol side). It should be mentioned that the inlet pressure for water and ethanol was 150 kPa.

The flow characteristics show that for very low flow rates the overall pressure drop was higher for the modified heat exchanger than for the commercial one. However this tendency was opposite for higher values of flow rates.

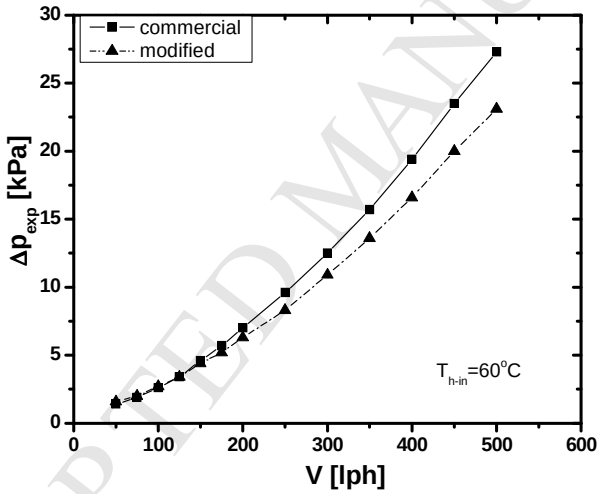

Fig. 10. Water side flow characteristics

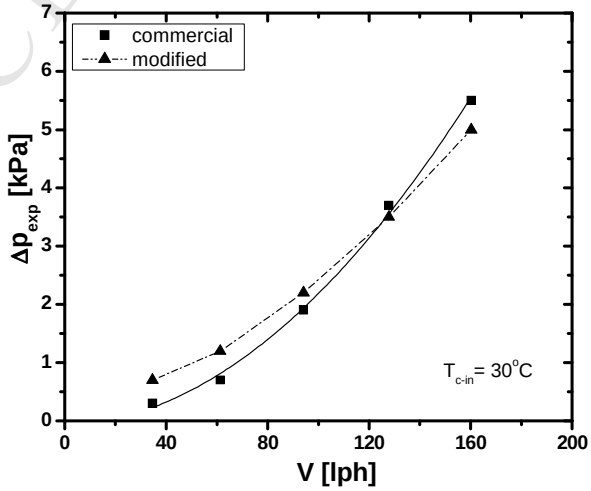

Fig. 11. Ethanol side flow characteristics

The smaller values of pressure drop on the heat exchanger water side could be partially explained with appearance of "apparent slip flow", which might contribute to reduction of shear stresses. The influence of increasing Reynolds number should be similar for the modified and commercial heat exchangers, that is why it was not taken into account in the interpretation of results. Considering the ethanol side, two clearly visible regions could be determined: (a) low Reynolds number, where pressure drop was higher for the modified heat exchanger and (b) higher Reynolds number – for which the pressure losses were lower for the modified heat exchanger. The explanation could be connected with the surface tension and wetting ability of ethanol. It looks like the porous layer caused higher pressure losses, because the ethanol penetrated "deeper" into the pores due to the smaller surface tension. However increasing Reynolds number caused reduction of boundary layer thickness, what lead to the reduction of pressure losses. The "apparent slip flow" seemed also to contribute to decreasing shear stresses. Of course, the Authors are aware that analyzed phenomena were not simple at all and there had to be the roughness influence on the hydrodynamic boundary layer, causing its unsteadiness. Unsteady boundary layer could be also a reason of smaller friction factor. This explanation is done to show how complex phenomena were occurring in the system and to said that they shouldn't be generalized with only the geometry influence. The fluid properties and flow structure are as important as the geometry itself. All mentioned parameters would have an impact on the final result, which might be enhanced or reduced.

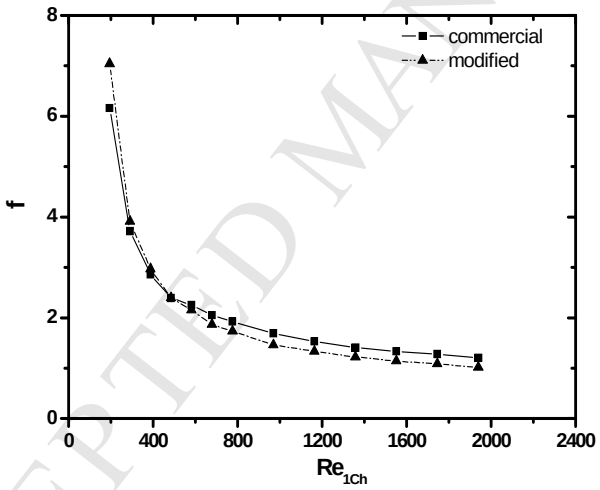

Fig. 12. Friction factor profile for water

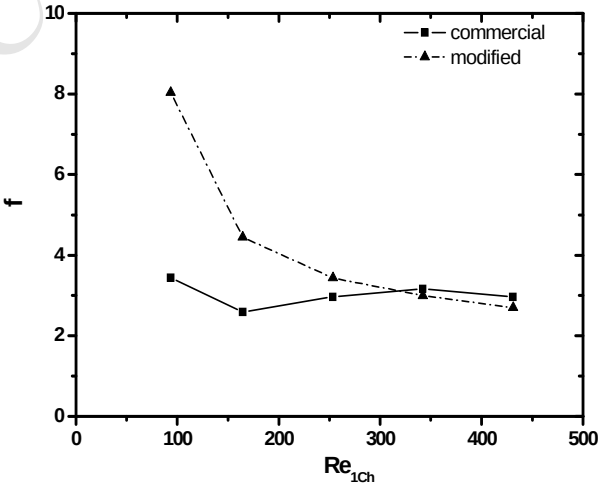

Fig. 13. Friction factor profile for ethanol

The apparent tendency in Figs. 10 and 11 corresponds to the friction factor presented as a function of the Reynolds number in Fig. 12 and Fig. 13. With increasing Reynolds number the friction factor of modified surface decreased and finally became smaller than for the commercial plate. At the Reynolds number equal to 93, the modified heat exchanger has 133% higher friction factor than the commercial one, while at the Reynolds number equal to 430 smaller than the commercial one of about 9%. For both fluids (water and ethanol) the partially linear region of friction factor dependence on the Reynolds number can be found, what the most probably corresponds to the transition region of the flow. According to Hesselgreaves [23] the range of transition from turbulent to laminar flow corresponds to the value of Re between 100 and 200. That means that in Fig. 12, in case of water, all data are for the turbulent flow regime, whereas in Fig. 13 the transition and turbulent flow regimes are present.

7. Uncertainty analysis

The uncertainty analysis of presented experimental investigations was done in systematic manner. Taking into account low number of measurements repetition, but also high repeatability of data, the statistic uncertainties were not considered. The analysis presented in this paper, concentrated on the systematic error analysis. The analysis was based on the principle of uncertainties propagation described by the formula [24]:

$$\Delta y = \sqrt{\left(\frac{\partial f}{\partial x_1}\Delta x_1\right)^2 + \left(\frac{\partial f}{\partial x_2}\Delta x_2\right)^2 + \left(\frac{\partial f}{\partial x_3}\Delta x_3\right)^2 + \ldots} \tag{21}$$

where Δx is the maximal uncertainty of measuring instrument. The uncertainty of analyzed functions depended on the particular variables uncertainties. In presented case the uncertainties were connected with direct measurements, indirect calculations and withdrawal from the tables (thermo-physical properties). The applied uncertainties of various devices used in experiment were described in the section discussing the experimental facility and procedure.
The results of uncertainties are summarized in Table 5. The relative uncertainty was calculated on the basis of the following equation:

$$\delta y = \frac{\Delta y}{y} \cdot 100\% \tag{22}$$

Table 5. Summary of the uncertainty analysis

Parameter	Relative value [%]
volumetric flow rate	0.92-1.13
mass flux	1.40-1.63
temperature	1.00-1.15
overall heat transfer coefficient	2.52-3.76
convective heat transfer coefficient	3.92-5.19
pressure	0.90-1.06
differential pressure	1.50-1.84
friction factor	4.91-6.23
Reynolds number	7.30-11.45

8. Summary

The experimental analysis of heat transfer enhancement for plate heat exchanger was described. The results of heat transfer for the exchanger with modified surface were always compared with the results of the commercial one. Analysis of water-ethanol system gave very interesting data – the heat transfer coefficient on the ethanol side took higher values for the modified heat exchanger in all studied cases, but the water side it was higher for the commercial one. That is due to the fact that the surface tension of ethanol was about four times smaller than the surface tension of water. Moreover the interaction of roughness with the hydrodynamical and thermal boundary layers was taken into account. The Prandtl number for ethanol was about three times higher than the one for water, what described the relation between particular boundary layers for both media. There should be mentioned one very important parameter related to the flow character, namely the flow regime: laminar, transitional or turbulent. The analyzed in the system phenomena were complex and it should be emphasized that the fluid properties and the flow structure are as important as the geometry itself. All mentioned parameters would have an impact on the final result (heat transfer coefficient, pressure losses, friction factor), which might be enhanced or reduced by the interaction of the parameters.

Acknowledgements

The investigations presented in the paper has been funded from the Strategic Research Programme SP/E/1/67484/10.

References

[1] T. Chen, J. Kim, H. Cho, Theoretical analysis of the thermal performance of a plate heat exchanger at various chevron angles using lithium bromide solution with nanofluid, Int. J. Refrig. 48 (2014) 233-244.

[2] A. Gupta, M. Uniyal, Review of heat transfer augmentation through different passive intensifier methods, IOSR J. Mech. Civ. Eng. 1 (2012) 14-21.

[3] K.M. Stone, Review of literature on heat transfer enhancement in compact heat exchangers, Air Conditioning and Refrigeration Center Technical Reports, 1996.

[4] M.M. Abu-Khader, Plate heat exchangers: Recent advances, Renew. Sust. Energ. Rev. 16 (2012) 1883– 1891.

[5] T.S. Khan, M.S. Khan, M.-C. Chyu, Z.H. Ayub, Experimental investigation of single phase convective heat transfer coefficient in a corrugated plate heat exchanger for multiple plate configurations, Appl. Therm. Eng. 30 (2010) 1058–1065.

[6] O. Arseneyeva, L. Tovazhnyansky, P. Kapustenko, G. Khavin, The generalized correlation for friction factor in crisscross flow channels of plate heat exchangers, Chem. Eng. Trans. 25 (2011) 399-404.

[7] D. Dovic, B. Palm, S. Svaic, Generalized correlations for predicting heat transfer and pressure drop in plate heat exchanger channels of arbitrary geometry, Int. J. Heat Mass Tran. 52 (2009) 4553–4563.

[8] Y. Islamoglu, C. Parmaksizoglu, The effect of channel height on the enhanced heat transfer characteristics in a corrugated heat exchanger channel, Appl. Therm. Eng. 23 (2003) 979–987.

[9] Y. Islamoglu, C. Parmaksizoglu, Numerical investigation of convective heat transfer and pressure drop in a corrugated heat exchanger channel, Appl. Therm. Eng. 24 (2004) 141–147.

[10] V.R. Naik, V.K. Matawala, Experimental investigation of single phase chevron type gasket plate heat exchanger, International Journal of Engineering and Advanced Technology (IJEAT) 2 (2013) 362-369.

[11] R. Furberg, B. Palm, S. Li, M. Toprak, M. Muhammed, The Use of a Nano- and Microporous Surface Layer to Enhance Boiling in a Plate Heat Exchanger, J. Heat Transfer 131 (2009) 101010-1-101010-8.

[12] H. Müller-Steinhagen, Smart Surfaces for Improved Heat Exchangers, (2008) HTRI e-publications, www.htrinet.com/ePubs/epubs.htm.

[13] A. García, J.P. Solano, P.G. Vicente, A. Viedma, The influence of artificial roughness shape on heat transfer enhancement: Corrugated tubes, dimpled tubes and wire coils, Appl. Therm. Eng. 35 (2012) 196-201.

[14] J. Wajs, D. Mikielewicz, Effect of surface roughness on thermal-hydraulic characteristics of plate heat exchanger, Key Eng. Mat. 597 (2014) 63-74.

[15] Personal communication with the company.

[16] W. Li, H. Li, G. Li, S. Yao, Numerical and experimental analysis of composite fouling in corrugated plate heat exchangers, Int. J. Heat Mass Tran. 63 (2013) 351–360.

[17] E.E. Wilson, A basis for rational design of heat transfer apparatus, Trans. ASME 37 (1915) 47-82.

[18] J. Fernandez-Seara, F.J. Uhia, J. Sieres, A. Campo, A general review of the Wilson plot method and its modifications to determine convection coefficients in heat exchange devices, Appl. Therm. Eng. 27 (2007) 2745-2757.

[19] Refprop v. 9.0, National Institute of Standards (NIST) (2010).

[20] Two Phase Flow, Phase Change and Numerical Modeling, ed. A. Ahsan, InTech, chapter: Ch. Choi, M. Kim, Wettability Effects on Heat Transfer, 2011. DOI: 10.5772/1043.

[21] S.G. Kandlikar, D. Schmitt, A.L. Carrano, J.B. Taylor, Characterization of surface roughness effects on pressure drop in single-phase flow in minichannels, Phys. Fluids 17 (2005) 100606; doi: 10.1063/1.1896985.

[22] R.K. Shah, D.P. Sekulic, Fundamentals of heat exchange design, John Wiley and Sons Inc., New York, 2003.

[23] J.E. Hesselgreaves, Compact heat exchangers, Selection, design and operation, Elsevier Science & Technology Books, 2001.

[24] R.J. Moffat, Describing the uncertainties in experimental results, Exp. Therm. Fluid Sci. 1 (1988) 3-17.

HIGHLIGHTS:

- Implementation of increased surface roughness into the plate heat exchanger
- Comparison between modified and commercially available plate heat exchanger
- Tested layer combined with ethanol gave higher heat transfer coefficient
- Ethanol high flow rates caused decrease of pressure drop
- Modified surface layer is suitable for fluids with low value of surface tension